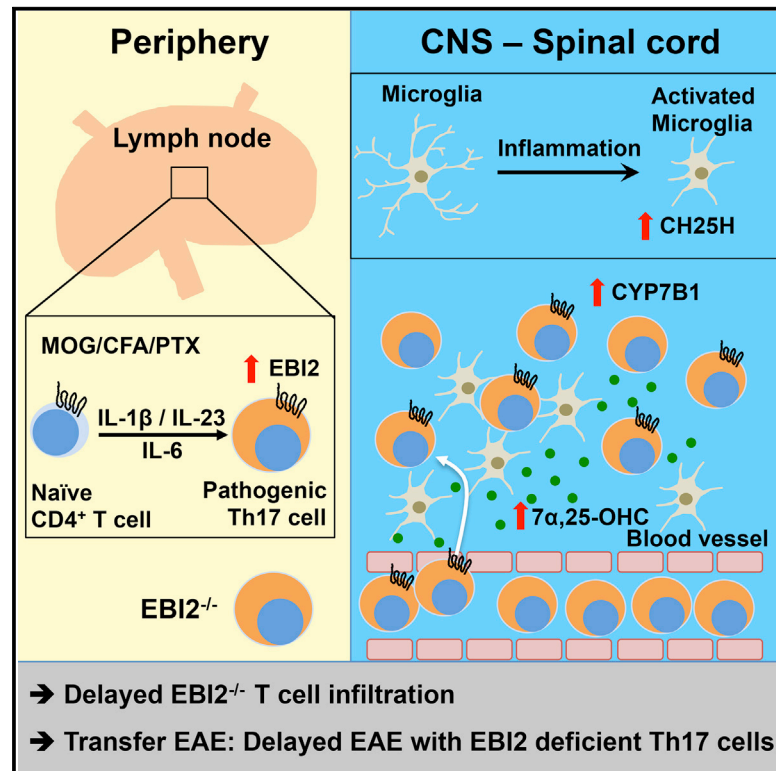Article

EBI2 Is Highly Expressed in Multiple Sclerosis Lesions and Promotes Early CNS Migration of Encephalitogenic CD4 T Cells

Graphical Abstract

Authors

Florian Wanke, Sonja Moos,
Andrew L. Croxford, ..., Stefano Casola,
Ari Waisman, Florian C. Kurschus

Correspondence

stefano.casola@ifom.eu (S.C.),
waisman@uni-mainz.de (A.W.),
kurschus@uni-mainz.de (F.C.K.)

In Brief

Wanke et al. show that EBI2 is expressed by Th17 cells in inflammation and that EBI2 promotes early CNS infiltration in passive EAE. Furthermore, they show that CH25H, CYP7B1, and 7α,25-OHC are upregulated in the CNS in EAE and that EBI2 expressing cells are highly present in MS lesions.

Highlights

- EBI2 in T cells is highly regulated and stabilized in Th17 cells by IL-1β and IL-23

- CH25H, CYP7B1, and 7α,25-OHC are elevated in the CNS in EAE

- EBI2 expression by Th17 cells promotes passive EAE

- Infiltrating cells in MS lesions express EBI2

CrossMark

CellPress

Article

EBI2 Is Highly Expressed in Multiple Sclerosis Lesions and Promotes Early CNS Migration of Encephalitogenic CD4 T Cells

Florian Wanke,[1] Sonja Moos,[1] Andrew L. Croxford,[1] André P. Heinen,[1] Stephanie Gräf,[1] Bettina Kalt,[1] Denise Tischner,[2] Juan Zhang,[3] Isabelle Christen,[3] Julia Bruttger,[1] Nir Yogev,[1] Yilang Tang,[1] Morad Zayoud,[1] Nicole Israel,[1] Khalad Karram,[1] Sonja Reißig,[1] Sonja M. Lacher,[1] Christian Reichhold,[1] Ilgiz A. Mufazalov,[1] Avraham Ben-Nun,[4] Tanja Kuhlmann,[5] Nina Wettschureck,[2] Andreas W. Sailer,[6] Klaus Rajewsky,[7] Stefano Casola,[8,*] Ari Waisman,[1,*] and Florian C. Kurschus[1,9,*]

[1]Institute for Molecular Medicine, University Medical Center of the Johannes Gutenberg-University Mainz, 55131 Mainz, Germany
[2]Max Planck Institute for Heart and Lung Research, 61231 Bad Nauheim, Germany
[3]Analytical Sciences and Imaging, Novartis Institutes for BioMedical Research, 4002 Basel, Switzerland
[4]Department of Immunology, The Weizmann Institute of Science, Rehovot, Israel
[5]Institute of Neuropathology, University Hospital Münster, 48149 Münster, Germany
[6]Chemical Biology & Therapeutics, Novartis Institutes for BioMedical Research, 4002 Basel, Switzerland
[7]Max-Delbrueck-Center for Molecular Medicine, 13125 Berlin-Buch, Germany
[8]IFOM–The FIRC Institute of Molecular Oncology, 20139 Milan, Italy
[9]Lead Contact
*Correspondence: stefano.casola@ifom.eu (S.C.), waisman@uni-mainz.de (A.W.), kurschus@uni-mainz.de (F.C.K.)
http://dx.doi.org/10.1016/j.celrep.2017.01.020

SUMMARY

Arrival of encephalitogenic T cells at inflammatory foci represents a critical step in development of experimental autoimmune encephalomyelitis (EAE), the animal model for multiple sclerosis. EBI2 and its ligand, 7α,25-OHC, direct immune cell localization in secondary lymphoid organs. CH25H and CYP7B1 hydroxylate cholesterol to 7α,25-OHC. During EAE, we found increased expression of CH25H by microglia and CYP7B1 by CNS-infiltrating immune cells elevating the ligand concentration in the CNS. Two critical pro-inflammatory cytokines, interleukin-23 (IL-23) and interleukin-1 beta (IL-1β), maintained expression of EBI2 in differentiating Th17 cells. In line with this, EBI2 enhanced early migration of encephalitogenic T cells into the CNS in a transfer EAE model. Nonetheless, EBI2 was dispensable in active EAE. Human Th17 cells do also express EBI2, and EBI2 expressing cells are abundant within multiple sclerosis (MS) white matter lesions. These findings implicate EBI2 as a mediator of CNS autoimmunity and describe mechanistically its contribution to the migration of autoreactive T cells into inflamed organs.

INTRODUCTION

Epstein-Barr virus-induced G protein-coupled receptor 2 (EBI2, also known as GPR183) was discovered in 1993 in a screen of genes induced by in vitro Epstein-Barr virus (EBV) infection of a Burkitt's lymphoma cell line (Birkenbach et al., 1993) and identified by sequence similarity as a G protein-coupled receptor (GPCR). EBI2 was shown to have an important role in B cell positioning in the germinal center reaction (Gatto et al., 2009; Pereira et al., 2009), resulting in fewer plasma cells and reduced antibody titers in EBI2-deficient animals. Also, CD4^{+} conventional dendritic cells (cDCs) are profoundly diminished in the spleen of EBI2 mutant mice (Gatto et al., 2013; Yi and Cyster, 2013). Recently, a role for EBI2 in differentiation of T follicular helper (Tfh) cells was demonstrated. Activated T cells were shown to migrate in an EBI2-dependent manner to the outer T zone to receive inducible T cell co-stimulator (ICOS) stimulation under IL-2 deprived conditions by IL-2 quenching DCs that fosters Tfh differentiation (Li et al., 2016). Furthermore, Suan et al. (2015) showed that Tfh cells in the germinal centers downregulate expression of EBI2. Thus, EBI2 regulates positioning of immune cells in secondary lymphoid organs.

Oxysterols were recently identified as natural ligands for EBI2 (Hannedouche et al., 2011; Liu et al., 2011). The most active ligand, 7α,25-dihydroxycholesterol (7α,25-OHC), is generated via sequential hydroxylation of cholesterol by cholesterol-25-hydroxylase (CH25H) and 25-hydroxycholesterol by 7-alpha-hydroxylase (CYP7B1). In naive mice, CH25H is highly expressed in the spleen, whereas CYP7B1 is expressed quite ubiquitously with highest expression in the liver. In addition, both enzymes are expressed in lymphoid stromal cells (Hannedouche et al., 2011; Yi et al., 2012). Contradictory data were published about the role of CH25H in experimental autoimmune encephalomyelitis (EAE) (Chalmin et al., 2015; Reboldi et al., 2014), and no direct contribution of EBI2 in EAE pathogenesis has been described.

Expression of EBI2 and its function for migration in vitro in T cells was recently reported (Chalmin et al., 2015; Hannedouche et al., 2011; Liu et al., 2011; Pereira et al., 2009). Pereira et al. (2009) used an EBI2 reporter mouse and found that most CD4^{+}

T cells, but only approximately half of the CD8$^+$ T cells, expressed EBI2. In vitro migration of murine T cell toward 7α,25-OHC was demonstrated previously (Chalmin et al., 2015; Liu et al., 2011).

To analyze EBI2 expression and its function in T cells in vivo, we created an EGFP reporter/knockout mouse strain, termed EBI2^{EGFP}. This mouse strain in heterozygous configuration allows for a systematic analysis of the expression of EBI2 in distinct cell types in steady-state and under inflammatory conditions. Among murine and human T cell subsets, EBI2 was highly and uniformly expressed by either naive CD4$^+$ T cells or within the Th17 subset under inflammatory conditions. Its expression was strongly repressed under transforming growth factor β (TGF-β) + interleukin-6 (IL-6)-induced Th17 differentiation conditions but sustained by interleukin-1 beta (IL-1β) and interleukin-23 (IL-23) during T helper cell differentiation. Strikingly, transfer of myelin oligodendrocyte glycoprotein (MOG)-specific EBI2-deficient Th17 cells isolated from homozygous EBI2$^{EGFP/EGFP}$ mice induced EAE with a significantly delayed onset. Moreover, we found that expression of the enzymes CH25H and CYP7B1 changes dramatically during the course of EAE with a strong up-regulation detected in the spinal cord (SC) leading to enhanced tissue levels of the EBI2 ligand in the SC in EAE. Additionally, we found that microglia start expressing CH25H early in EAE and that CYP7B1 is expressed in EAE by infiltrating monocytes and lymphocytes. In accordance with our mouse data, EBI2 was highly expressed by human Th17 cells derived from peripheral blood mononuclear cells (PBMCs). Furthermore, macrophages and a subset of T cells in lesions of multiple sclerosis (MS) patients stained positive for EBI2. Therefore, we suggest that EBI2 and its ligand(s) play important roles for efficient and early migration of encephalitogenic CD4$^+$ T cells into the CNS. This mechanism may also be more generally implicated in the infiltration of human lymphocytes into inflamed tissues.

RESULTS

EBI2 Expression in T Cells Regulates Their Migration

To systematically study the expression of EBI2 in the immune system, we replaced the single coding exon of the *EBI2/Gpr183* gene with the EGFP minigene, resulting in loss of EBI2 and EGFP expression under the control of *EBI2 cis* regulatory elements (Figures S1A and S1B).

Using this reporter system (targeted mutation in heterozygous configuration), we investigated expression of EBI2 in both CD4$^+$ T cells and cytotoxic CD8$^+$ T cells. The majority of naive CD4$^+$ T cells, but only a small fraction of naive CD8$^+$ T cells, expressed EBI2 (Figure 1A). The frequency of EGFP$^+$ cells was reduced in memory/effector (CD44^{hi}CD62L^{lo}) T cells (Figure 1B) as compared to naive T cells. Conversely, a high proportion of central memory (CD44^{hi}CD62L^{hi}) CD8$^+$ T cells showed strong expression of EBI2 (Figure 1B). The intensity of EGFP fluorescence correlated with *Gpr183* mRNA expression in sorted EGFP$^+$ CD4$^+$ T cells (Figure 1C) as well as sorted EGFP-positive effector T cells from EBI2$^{EGFP/+}$ heterozygous mice (Figure S1C).

7α,25-OHC was identified as the most potent EBI2 ligand (Hannedouche et al., 2011; Liu et al., 2011). In line with the EBI2 expression levels, CD4$^+$ T cells migrated more efficiently

toward 7α,25-OHC than CD8$^+$ T cells (Figures 1D and S1D). EBI2-deficient T cells from EBI2$^{EGFP/EGFP}$ mice did not migrate toward the ligand, excluding EBI2-independent chemotaxis to 7α,25-OHC (Figures 1D and S1D). In line with recent data (Chalmin et al., 2015), increasing concentrations of 7α,25-OHC inhibited migration of wild-type (WT) T cells, likely because of EBI2 internalization. We further analyzed the migratory behavior of EBI2-deficient T cells toward the CCR7 ligands CCL19/CCL21 and found it comparable to WT T cells (Figure S1E). Interestingly, pre-treatment of T cells with 1 μM of 7α,25-OHC also significantly decreased migration toward CCL19 and CCL21 (Figure S1F), a phenomenon known as heterologous desensitization (Kelly et al., 2008), which was previously shown for B cell migration induced by various chemokines (Liu et al., 2011). However, in transfer experiments with EBI2-deficient T cells, we did not detect differences in homing to peripheral lymphoid organs (Figures S1G and S1H).

EBI2 Expression in T Helper Cell Subsets

As we detected reduced proportions of EBI2 expressing T cells among effector/memory-type T cells (Figure 1B), we further analyzed the cytokine expression profiles of EBI2-expressing Th subsets. In non-immunized mice, we found $\sim$40% of Th1 (interferon-gamma positive [IFN-$\gamma$$^+$]), Th17 (interleukin-17A positive [IL-17A$^+$]), and FoxP3$^+$ regulatory T cells expressing EBI2 (Figure 1E). Importantly, we did not detect any significant differences in quantity of Th1, Th17, and Treg cells in EBI2-deficient mice compared to control mice (Figure 1F).

To assess EBI2 expression of in vitro differentiated T cell subsets, we polarized naive T helper cells under different conditions. In contrast to the ex vivo findings, most in vitro differentiated FoxP3$^+$ Tregs expressed EBI2 (Figure 2A). In the presence of IL-2, EBI2 expression was partially decreased (Figures 2A and 2B). Furthermore, Th17 cells differentiated in vitro with TGF-β1 and IL-6 showed only weak expression of EBI2 (Figure 2C), whereas in vitro differentiated Th1 cells were more comparable to ex vivo Th1 cells (Figure 1E), showing a bimodal expression profile of the EBI2-EGFP reporter (Figure 2C).

It was recently shown that signaling via the S1P(1) receptor influences the balance between Th1 and regulatory T cells (Liu et al., 2010). Therefore, we speculated that EBI2-signaling via 7α,25-OHC might similarly influence T cell differentiation. However, we did not find any effect on in vitro T cell differentiation to induced Tregs, Th17, or Th1 cells when 7α,25-OHC was added (Figures 2C and S2B). In line with this, EBI2 deficiency did not impair in vitro T cell differentiation (Figures S2A and S2B).

EBI2 Deficiency on APCs or on T Cells Has No Major Impact on Priming of Encephalitogenic T Cells

It was recently shown that EBI2 is highly expressed by CD4$^+$ cDCs in the spleen and that this subset is strongly diminished in mice deficient for either EBI2 or CH25H (Gatto et al., 2013; Yi and Cyster, 2013). As we observed the same deficiency in our EBI2-deficient mice (data not shown), we reasoned that it might influence priming of T cells in peripheral lymphoid organs. To test this hypothesis, we adoptively transferred purified carboxyfluorescein succinimidyl ester (CFSE)-labeled CD4$^+$ T cells from mice expressing a transgenic T cell receptor specific to
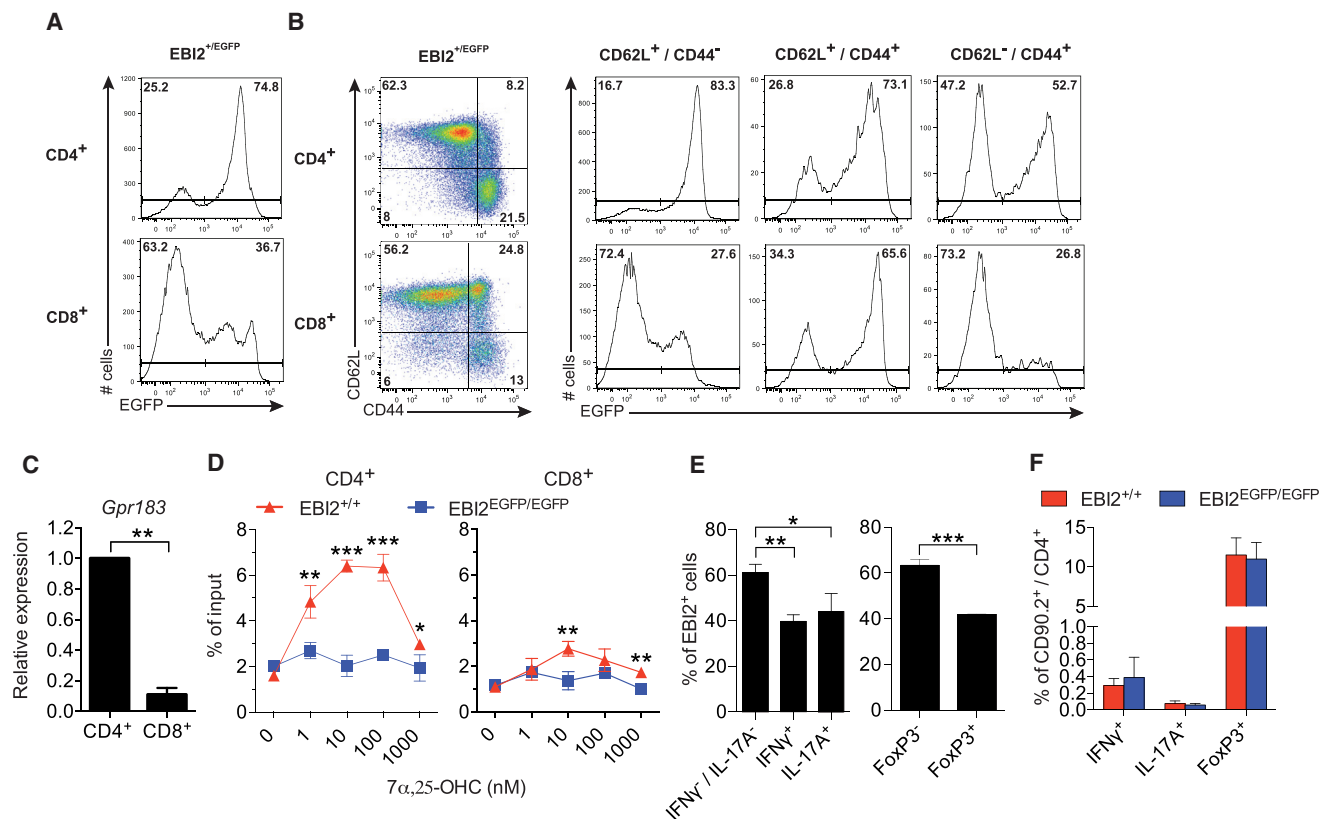
Figure 1. Differential Expression of EBI2 on T Cell Subsets

(A) Flow cytometric analysis of EBI2-EGFP expression in gated CD4$^+$ and CD8$^+$ T cells in LNs of EBI2$^{+/EGFP}$ mice.

(B) Flow cytometric analysis of EBI2-EGFP expression in different T cell subsets (right) in LNs of EBI2$^{+/EGFP}$ animals, according to CD62L and CD44 expression (left). Numbers in histograms indicate the percentage of cells in the respective gates. Shown are representative plots for at least three independent experiments (n = 3).

(C) Relative expression of *Gpr183* mRNA of MACS-purified CD4$^+$ and CD8$^+$ T cells from EBI2$^{+/+}$ mice by qRT-PCR. Expression was normalized to *Hprt* mRNA expression and the value of CD4$^+$ T cell was set to 1.0. Shown is the mean with SD of two independent experiments (n = 2).

(D) Transwell migration assay of α-CD3- and α-CD28-activated splenocytes toward indicated concentrations of 7α,25-OHC. Migrated CD4$^+$ and CD8$^+$ T cells were quantified by flow cytometry. Shown are means with SD of technical replicates representative of at least three independent experiments.

(E) Statistical analysis of EBI2-EGFP expression in IFN-γ$^-$IL-17A$^-$ T helper cells and Th1 (IFN-γ$^+$IL-17A$^-$), Th17 (IL-17A$^+$IFN-γ$^-$) (left panel), and conventional (FoxP3$^-$) versus regulatory (FoxP3$^+$) T cells of naive EBI2$^{+/EGFP}$ mice (right panel). Data is representative of at least two independent experiments (n = 3).

(F) Flow cytometric quantification of Th1, Th17, and regulatory T cells in LNs of naive EBI2-deficient (EBI2$^{EGFP/EGFP}$) mice or littermate controls.

MOG$_{35–55}$ (2D2 mice, expressing the congenic marker CD90.1) into EBI2-deficient hosts or wild-type littermates (both expressing the congenic marker CD90.2). One day post transfer, host mice were immunized subcutaneously (s.c.) with MOG$_{35–55}$ emulsified in complete Freund's adjuvant (CFA) or left untreated. Transferred T cells in lymph nodes (LNs) and spleen (data not shown) were analyzed 5 days post immunization for CFSE dilution and expression of CD62L and CD44. However, we could not detect significant differences in proliferation or activation of the transferred T cells in LNs (Figures S3A and S3B) or spleen (data not shown), suggesting that the reduced number of CD4$^+$ splenic DCs does not influence priming of MOG-specific T cells.

To test whether EBI2 deficiency on T cells would affect early priming on encephalitogenic 2D2 T cells, we also did the reciprocal experiment. To this end, we transferred cell tracer-labeled EBI2-sufficient and -deficient 2D2 T cells into congenic hosts and immunized the latter with MOG$_{35–55}$ in CFA. Again, we could

neither detect differences in T cell proliferation, nor in activation in the draining LNs (Figures S3C and S3D). These data indicate that EBI2 deficiency does not impair priming of T cells against the MOG$_{35–55}$ peptide.

EBI2 Is Highly Expressed by Inflammatory Th17 Cells

As CH25H-deficient mice show a delayed onset of EAE (Chalmin et al., 2015), we reasoned that EBI2 deficiency would also influence the migration properties of pathogenic T helper cells to the target tissue. In contrast to the data obtained with CH25H-deficient mice, EBI2$^{EGFP/EGFP}$ mutant animals were as susceptible to EAE induction as control littermates (Figure 3A). This was also confirmed by similar numbers of CD4$^+$ T cells infiltrating the CNS of control and EBI2 mutant mice, as seen by flow cytometric (Figures 3B and 3C) and histological (data not shown) analysis. In addition, we did not find any changes in the proportion of Th1, Th17, or regulatory T cells invading the CNS of
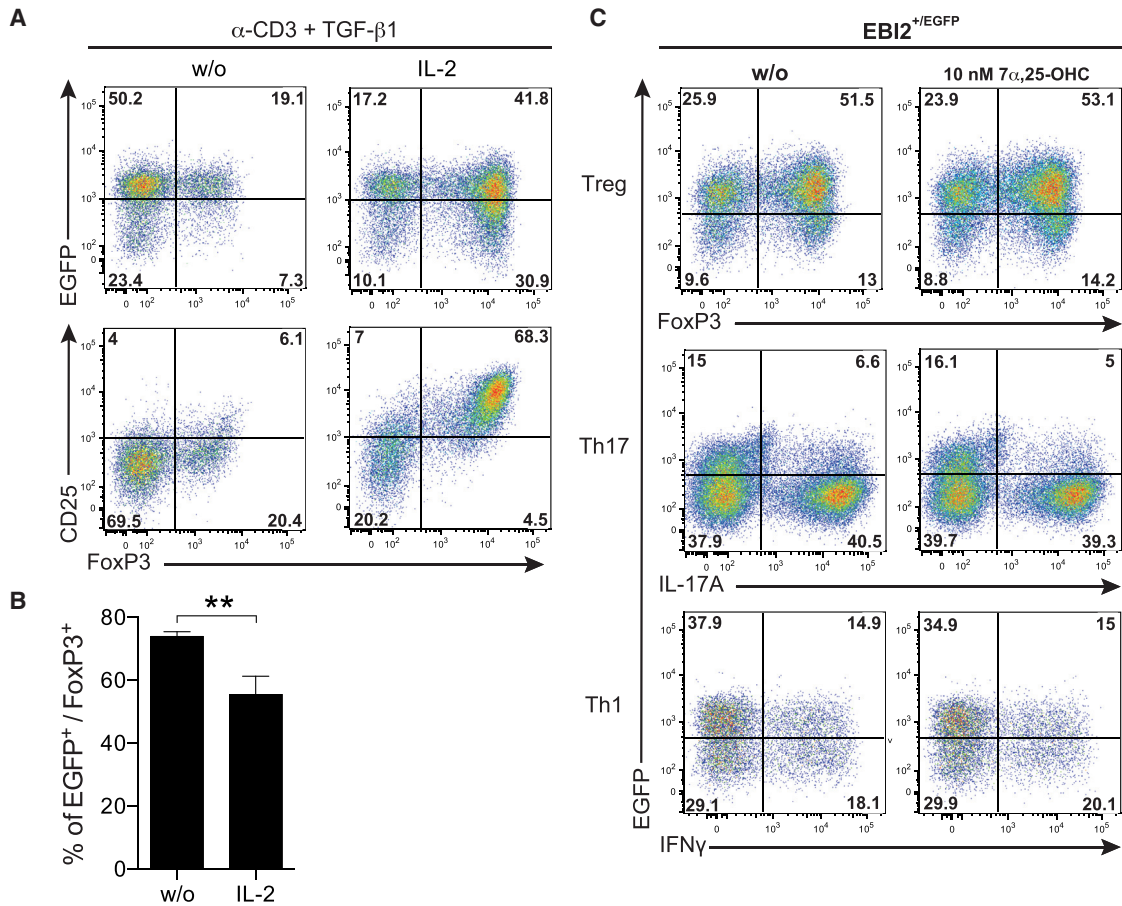
Figure 2. Differential Expression of EBI2 in T Cell Subsets

(A) Analysis of EBI2 expression of in vitro differentiated regulatory T cells from EBI2$^{+/EGFP}$ mice in the presence or absence of 10 ng/mL IL-2. Cells were gated as CD4$^+$ live cells.

(B) Statistical analysis of EGFP$^+$ regulatory T cells from EBI2$^{+/EGFP}$ mice after in vitro differentiation in the presence or absence of 10 ng/mL IL-2.

(C) Flow cytometric analysis of EBI2-EGFP expression of in vitro differentiated Th1, Th17, and iTreg cells from EBI2$^{+/EGFP}$ mice, in the presence or absence of 10 nM 7α,25-OHC. Cells were gated as CD4$^+$ live cells.

EBI2-deficient mice (Figure 3B) during active EAE. However, when we analyzed the patterns of EBI2 expression by different effector T cells in the inflamed CNS, we found a significantly higher frequency of EBI2-expressing Th17 cells (∼85%) as compared to LNs (∼50%) of mice with EAE (Figures 3D and 3E). In addition, the frequency of EBI2-expressing Th17 cells in LNs of mice with EAE was slightly increased compared to those of naive, non-immunized animals (∼40% Figure 1E).

IL-1β has been associated with differentiation of pathogenic T cells in both mice and humans (Acosta-Rodriguez et al., 2007; Chung et al., 2009; Croxford et al., 2015), and it was recently reported that T cells that differentiated in vitro with IL-6, IL-1β, and IL-23 are highly pathogenic compared to TGF-β1 and IL-6 polarized Th17 cells (Ghoreschi et al., 2010). IL-23 has been shown to play a pivotal role for pathogenicity in both conditions (Lee et al., 2012). Here, we found that Th17 cells polarized with IL-6 and TGF-β lost EBI2 expression during differentiation. The addition of IL-23 to the culture partially sustained EBI2 expression in Th17 cells differentiated in vitro

(Figures 3F and 3G). Maintenance of EBI2 expression was most visible when Th17 cells were differentiated using a combination of IL-6, IL-1β, and IL-23. Therefore, we propose that IL-1β, together with IL-23, maintains or even enhances EBI2 expression on Th17 cells under inflammatory conditions during EAE. Finally, in accordance with data from reporter animals, analysis of *Gpr183* expression by single cell RT-PCR confirmed that conventional as well as regulatory T cells express EBI2 mRNA at enhanced frequencies under inflammatory conditions (Figure 3H).

EBI2 Expression Confers Pathogenicity to Myelin-Specific Th17 Cells

Given our findings that Th17 cells express EBI2 more uniformly than Th1 cells, we reasoned that they might be more responsive to EBI2-mediated chemotaxis. Therefore, we analyzed the pathogenicity of EBI2-deficient Th17 cells in an adoptive transfer model of EAE. Strikingly, when we transferred Th17 cells lacking EBI2 into RAG1$^{-/-}$ hosts, onset of EAE was significantly delayed
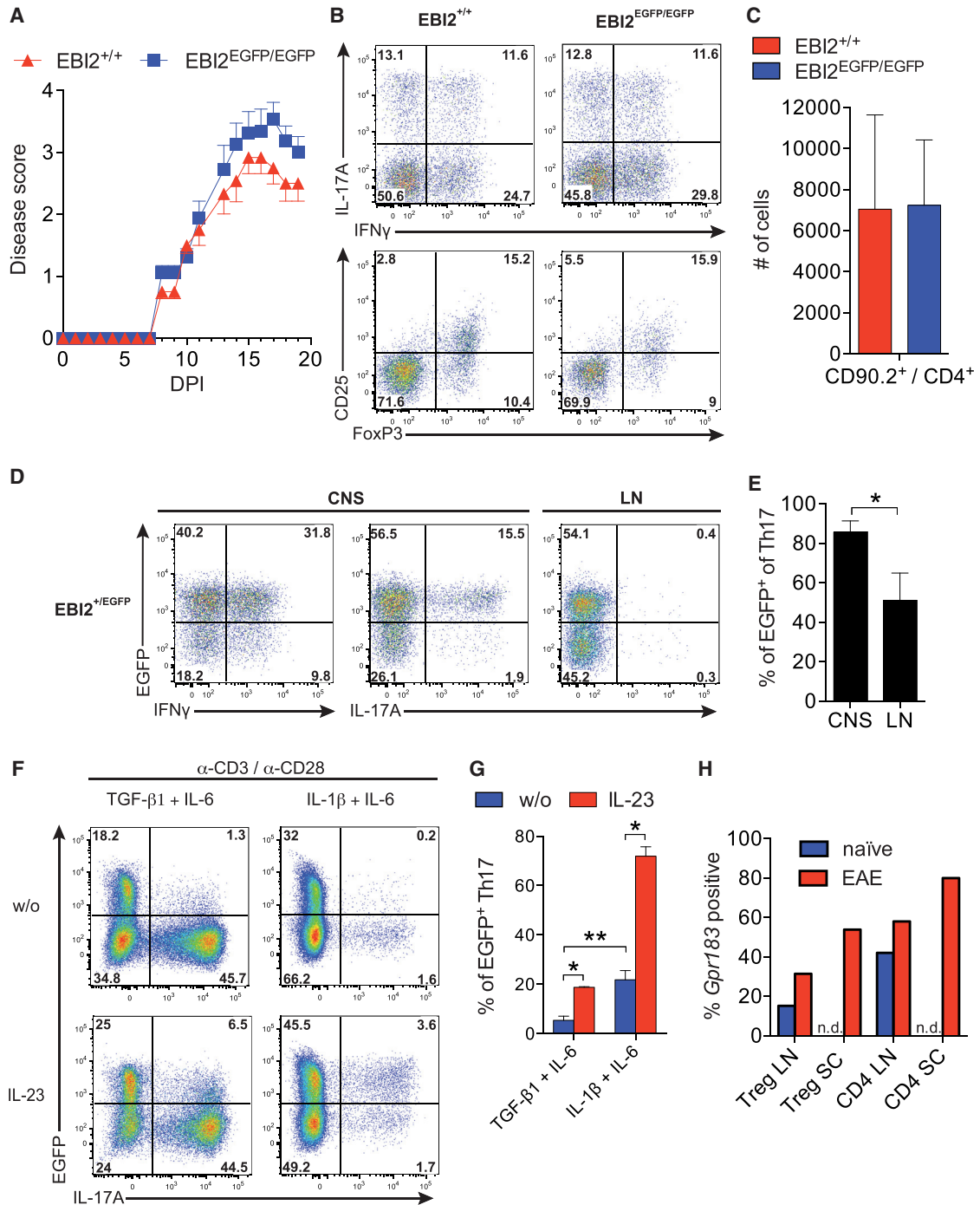
Figure 3. EBI2 Is Induced under Inflammatory Settings

(A) EAE development in EBI2$^{+/+}$ and EBI2$^{EGFP/EGFP}$ mice after immunization (n = 8). Data are representative of three independent experiments including one based on the use of a different EBI2 mutant strain (Table S1).

(B) IL-17A- and IFN-γ-expressing T helper cells and regulatory T cells in the CNS of EBI2$^{+/+}$ and EBI2$^{EGFP/EGFP}$ mice during EAE.

(C) Quantification of infiltrating CD4$^+$ T cells in the CNS of EBI2$^{+/+}$ and EBI2$^{EGFP/EGFP}$ mice with EAE.

(D) Flow cytometric analysis of EBI2-EGFP expression in IL-17A- and IFN-γ-secreting T helper cells within the CNS or LNs of EBI2$^{+/EGFP}$ mice with EAE.

(E) Statistical analysis of EGFP$^+$ Th17 cells in the CNS and LNs of EBI2$^{+/EGFP}$ mice with EAE. Data are representative of at least three independent experiments.

(F) EBI2-EGFP expression of in vitro differentiated Th17 cells using either TGF-β1 or IL-1β in combination with IL-6, in the presence or absence of IL-23.

(legend continued on next page)

(Figures 4A–4C). On average, we observed a delay of ∼4 days between transfer EAE induced by EBI2-deficient T cells to that with control T cells (Figures 4A–4C; Table S2). In line with this, we noted a significant reduction in the numbers of CD4$^+$ T cells in the CNS of the mice that received EBI2-deficient Th17 cells compared to those that were inoculated with control T cells (Figure 4D). At early time point analysis at day 15, we found that a lower proportion of the infiltrating T cells of EBI2-deficient mice expressed granulocyte-macrophage colony-stimulating factor (GM-CSF), whereas the expression of other cytokines was not significantly different. Furthermore, absolute numbers of all T helper cell populations were reduced significantly at day 15 (Figures 4E and S4A). Later time point analysis at day 28 post transfer showed that infiltration of CD4$^+$ T cells and their cytokine expression profile became comparable between knockout and control T cell transfers (Figures S4B and S4C). Similar to what we previously reported (Kurschus et al., 2010), analysis of cytokine expression of infiltrating T cells showed that many of the transferred Th17 cells from both controls and EBI2-deficient mice re-differentiated to IFN-γ and GM-CSF-producing cells. This was true for early (day 15) as well as late time points (day 28) (Figures 4E and S4B, respectively). Like in active EAE, we found higher frequencies of EBI2-expressing Th17 cells in the CNS when compared to that within the T cell mixture prior to transfer or in peripheral LNs at the time of analysis on day 28 post transfer (Figures 4F and 4G). Comparison of different cytokine-expressing T cell populations at day 28 in transfer EAE showed that those T cells expressing multiple cytokines such as IL-17A and IFN-γ or GM-CSF expressed EBI2 at the highest proportion (Figures S4D and S4E). These findings suggest a role for EBI2 in the early migration of encephalitogenic Th17 cells from peripheral lymphoid organs to the CNS.

To investigate whether T cells lacking EBI2 might be less able to infiltrate the CNS parenchyma, we performed immunohisto-chemistry. We stained for CD3-positive T cells at day 16 post transfer when EAE had just started in mice receiving EBI2-deficient T cells (Figure S4F). The lesions we found in mice transferred with EBI2-deficient T cells did not show major qualitative differences in terms of T cell migration into the tissue. We did not observe a stronger accumulation of EBI2-deficient T cells in the perivascular space compared to control T cells. These results therefore rather point to delayed infiltration kinetics but not to a major deficit in the capability of endothelial and blood brain barrier transmigration.

To examine whether priming in the LNs under inflammatory conditions has an impact on EBI2 expression in vivo, we analyzed encephalitogenic 2D2-EBI2^{EGFP} cells after transfer in WT hosts, which were subsequently immunized with MOG/CFA. Analysis at day 5 post immunization revealed that 2D2 T cells upregulated EBI2 consecutively during their proliferation (Figures 4H and 4I). This shows that EBI2 is dynamically regu-lated and is present at high levels on T cells, which have undergone their priming and proliferation phase in the LNs.

In order to determine whether the encephalitogenic T cells of EBI2-deficient mice were indeed less able to transmigrate into the CNS, we co-transferred encephalitogenic WT and EBI2-deficient cells (1:1) into RAG1$^{-/-}$ mice (Figure 5A). Those settings allowed tracking of in vitro expanded WT as well as EBI2-deficient Th17 cells within the same host. We analyzed animals at an EAE score between 1 and 2. The ratio of WT to EBI2-deficient total T cells was largely maintained in the spleen and in blood but changed in the CNS in favor of the EBI2 expressing WT T cells (Figures 5B and 5C). Interestingly, both Th1 as well as Th17 cells showed in spleen and blood a higher proportion of EBI2-deficient T cells but an inversed ratio in the CNS (Figure 5C). This data are in line with a reduced capacity of encephalitogenic effector T cells of EBI2-deficient mice to transmigrate into the CNS.

To test whether and how lack of EBI2 would affect proliferation and distribution of defined antigen-specific T cells under active EAE priming conditions, we co-transferred 2D2 T cells, either sufficient or deficient for EBI2 into congenic CD45.1$^+$ hosts that were subsequently immunized and analyzed at day 9 post immunization (Figure 5D). At day 9, we could recover only minute amounts of transferred T cells in most spleens of immunized hosts (data not shown) but proliferated cells of both genotypes were readily detected in equal numbers in the LNs (Figures 5E and 5F). Interestingly, proliferated EBI2-deficient 2D2 cells accumulated in the blood when compared to EBI2 sufficient T cells. In some mice, the ratio of EBI2-deficient 2D2 T cells over WT-2D2 T cells reached 10- to 20-fold. This ratio change was true for total 2D2 T helper cells as well as for Th17 cells (Figures 5E, 5F, S5A, and S5B). To date, we cannot explain the discrepancy between this and the transfer experiment (Figure 5C), in which only a small non-significant overrepresentation of EBI2-deficient T cells was found in the blood. This might be due to the difference of both settings used (active versus passive EAE), the transgenic T cell receptor used, or due to the different timing of both experiments.

Enzymes Involved in 7α,25-OHC Generation Are Upregulated in the CNS during EAE Progression

The observed effect of EBI2 deficiency on transfer EAE prompted us to analyze whether the enzymes involved in the generation of 7α,25-OHC (Figure 6A) were upregulated at the onset of EAE in the CNS. We quantified mRNA levels for the different enzymes involved in EBI2 ligand synthesis in tissue of naive mice and of littermates 10 days after EAE induction. In naive mice, *Ch25h* transcripts were expressed at low levels in the CNS. Strikingly, following immunization, expression of *Ch25h* and *Cyp7b1* was significantly upregulated in the SC of the animals (Figure 6B). In contrast, expression of the EBI2 ligand-degrading enzyme *Hsd3b7* was reduced (Figure 6B). This suggests that

(G) Statistical analysis of EBI2 expression in Th17 cells differentiated in vitro under indicated conditions. Data are representative of three or more independent experiments.

(H) Single cell RT-PCR analysis of the percentage of *Gpr183* expressing CD4$^+$ Th cells (CD4) and FoxP3-positive regulatory T cells (Treg) from LN or SC of healthy (blue) or EAE-induced (red) mice (n = 26–124 cells per group; see the Supplemental Experimental Procedures for details). N.d., not determined.
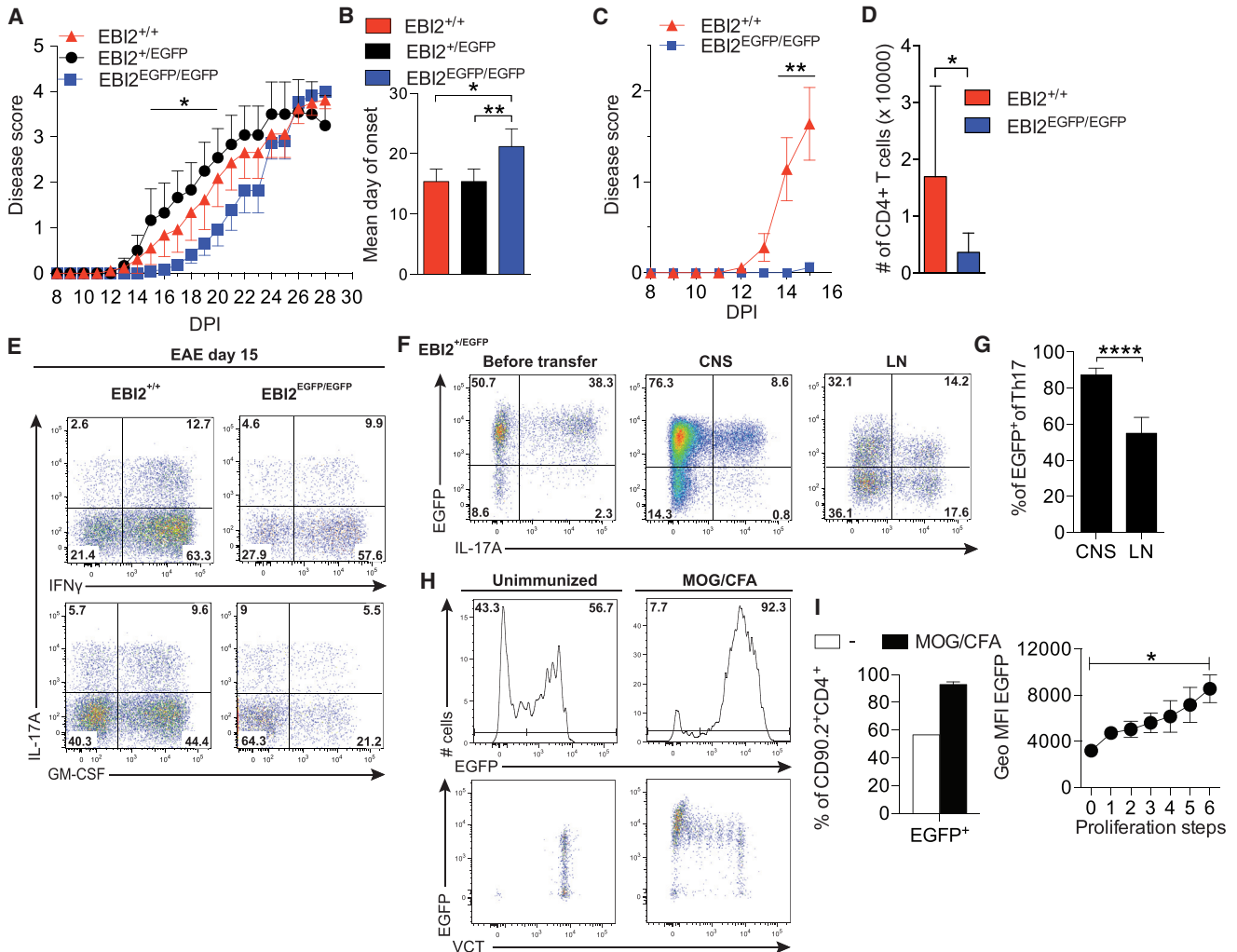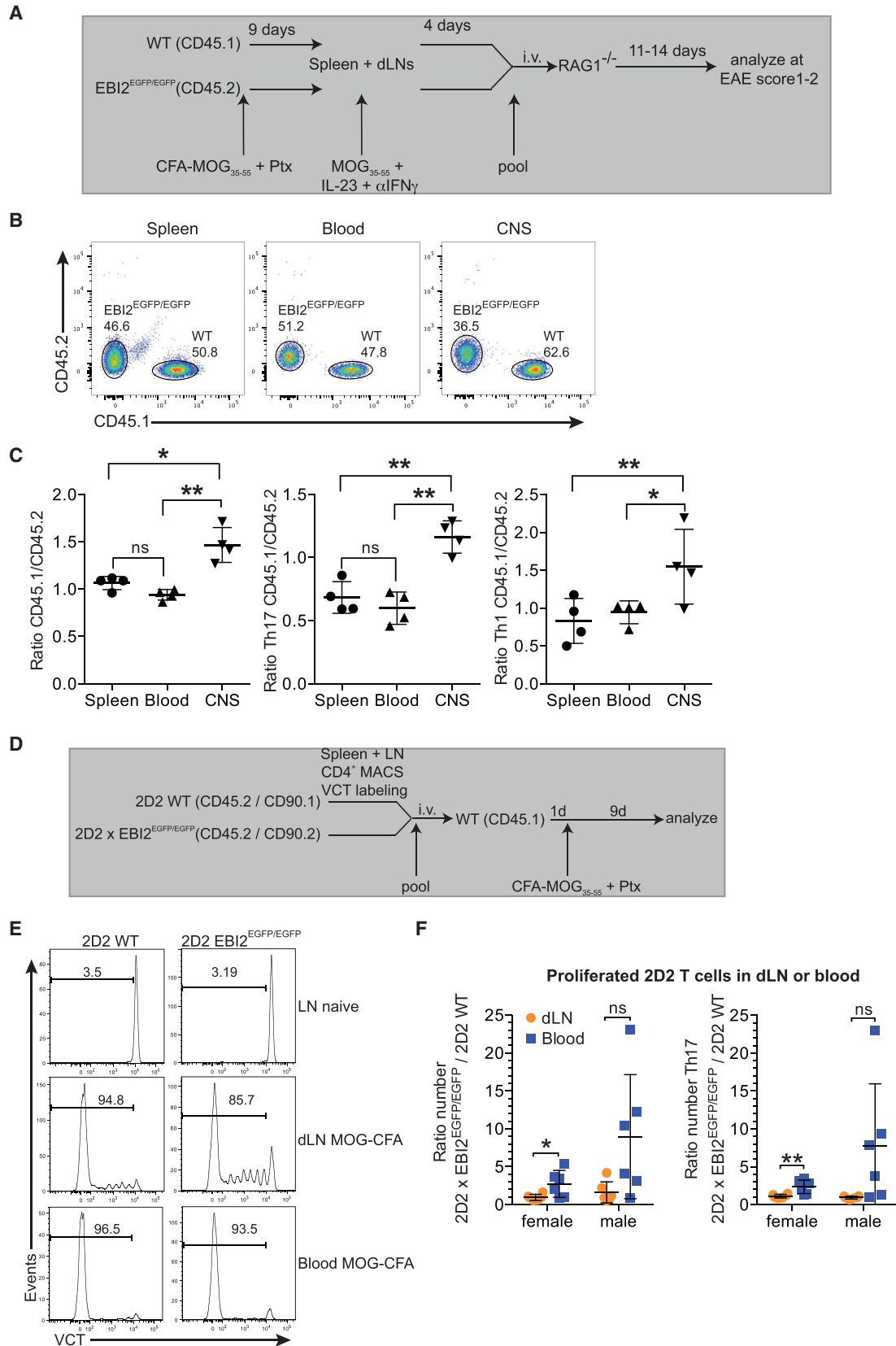
Figure 4. Delayed Onset of Transfer EAE with T Cells Deficient for EBI2

(A) EAE development of RAG1-deficient mice transferred with Th17 cells from indicated mice. The curve shows the mean with SEM (n = 6-11). EAE was terminated on day 28.

(B) Mean day of onset from two different experiments pooled (lasting 28 days).

(C) Disease development of RAG1$^{-/-}$ mice receiving Th17 cells from mice of the indicated genotypes (mean with SEM, n = 9). EAE was terminated on day 15.

(D) Quantification of T helper cells within the CNS on day 15 post transfer.

(E) Cytokine-expressing CD4 T cells in CNS on day 15 post transfer.

(F) EBI2-EGFP expression of Th17 cells before transfer and within the CNS and LNs on day 28 post transfer.

(G) Statistical analysis of EGFP$^+$ Th17 cells in the CNS or LNs. Data are representative of at least three independent experiments (see also Table S2).

(H) EGFP expression of purified and VCT-labeled helper T cells from 2D2 x EBI2$^{+/EGFP}$ mice. Cells were transferred into congenic WT mice, which were immunized with MOG/CFA or left untreated. Cells in the LNs were analyzed on day 5 post immunization.

(I) Statistical analysis of EGFP$^+$ helper T cells after immunization. Geometrical mean fluorescence (GeoMFI) of EBI2-EGFP in helper T cells in relation to the number of proliferation steps. Data are representative of two independent experiments.

concentrations of 7α,25-OHC are low in the CNS of naive mice but upon EAE induction, 7α,25-OHC synthesis becomes abundant in the CNS. To validate this assumption, we measured the EBI2 ligand 7α,25-OHC as well as other di- and monohydroxy-cholesterols in the SCs of naive mice and of sick mice in two different EAE groups, one at day 16 with a low grade EAE (average score 1.25 at the time of analysis) and another one at day 21 EAE (average score 2.6 at the time of analysis). In line with the upregulated enzymes, we found that 7α,25-OHC was

significantly upregulated in the SC of mice with EAE, and in the group with stronger EAE, we also observed higher levels of the ligand (Figure 6C). Furthermore, the dihydroxycholesterols 7α,27-OHC (the second best EBI2 ligand defined by now) and 7α,24-OHC showed higher levels to varying degrees in SCs of mice with EAE than of naive mice (Figure S6). The monohydroxycholesterol 25-OHC was also upregulated, whereas 27-OHC and 24-OHC were present at lower levels in diseased mice compared to naive mice (Figure S6).

A

WT (CD45.1) —9 days→ Spleen + dLNs —4 days→ i.v.→ RAG1⁻/⁻ —11-14 days→ analyze at EAE score1-2

EBI2^EGFP/EGFP (CD45.2) →

CFA-MOG₃₅₋₅₅ + Ptx   MOG₃₅₋₅₅ + IL-23 + αIFNγ   pool

B

Spleen | Blood | CNS

C

D

Spleen + LN
CD4⁺ MACS
VCT labeling

2D2 WT (CD45.2 / CD90.1) → i.v.→ WT (CD45.1) —1d—9d→ analyze

2D2 x EBI2^EGFP/EGFP (CD45.2 / CD90.2) →

pool   CFA-MOG₃₅₋₅₅ + Ptx

E

2D2 WT | 2D2 EBI2^EGFP/EGFP

F

Proliferated 2D2 T cells in dLN or blood

(legend on next page)

Microglia Express CH25H during EAE

It was recently suggested that infiltrating monocytes/macrophages might express the enzymes necessary to produce the EBI2 ligand in EAE (Chalmin et al., 2015). To test this, we sorted lymphocytes as well as microglia and different infiltrating myeloid cell populations from mice with EAE. To unambiguously ensure that the microglia gate did not contain infiltrating monocytic populations, we used a recently published mouse model for FACS, in which microglia are marked by an EYFP reporter (Cx3cr1CreER x Rosa-EYFP mice) (Bruttger et al., 2015; Yona et al., 2013). Only EYFP-positive microglia and EYFP-negative infiltrating myeloid cells were sorted (Figures 6D and 6E). We found that in EAE, microglia strongly expressed *Ch25h* mRNA, whereas infiltrating cells such as lymphocytes, monocytes, or monocyte-derived DCs (moDCs) did express *Ch25h* only at very low levels. On the other hand, the second important enzyme in generating the EBI2 ligand, *Cyp7b1*, was expressed by infiltrating lymphocytes and monocytes but not by microglia. *Hsd3b7* mRNA was found in microglia as well as in infiltrating myeloid populations (Figure 6F). We also sorted microglia from naive and EAE mice, and in line with the total tissue analysis, we found that in microglia *Ch25h* was expressed only in EAE and not in the healthy CNS (Figure 6G).

Human Th17 Cells Express EBI2

As we found that EBI2 expression is associated with the pathogenicity of murine Th17 cells, we also analyzed its expression in human cells by using a monoclonal antibody specific for human EBI2. Staining of human PBMCs from healthy donors revealed that EGFP expression in our reporter mice reflected very well expression of EBI2 by human T cells. Indeed, the majority of CD4+ T cells expressed EBI2 in contrast to CD8+ T cells (Figures 7A–7C and S7A). However, in contrast to the mouse data, EBI2 expression was uniformly higher on effector (CD45RA−) than on naive (CD45RA+) T helper cells (Figures 7A and S7B). In line with the in vitro migration assay of murine T cells, high concentrations of 7α,25-OHC reduced EBI2 cell surface expression (Figures 7A and S7C) to background levels (Figure 7C). When we analyzed cytokine-secreting T cells, we found that Th17 cells expressed higher levels of EBI2 compared to Th1- or IFN-γ- expressing CD8+ T cells (Figures 7D and 7E) both in percentage as well as in mean fluorescence intensity. Similar to mouse CD4+ T cells, human T helper cells from healthy blood donors migrated to 7α,25-OHC in a dose-dependent manner and high concentrations of the ligand inhibited migration (Figure 7F). Furthermore,

migration to the EBI2 ligand could be largely diminished by pre-incubation of the T cells with the EBI2 antagonist NIBR189 (Gessier et al., 2014) (Figure 7G).

To investigate whether EBI2 might also play a role in MS, we analyzed EBI2 expression in MS lesions. Strikingly, histological analysis revealed high expression of EBI2 in the inflamed white matter, in contrast to non-affected white matter regions (Figure 7H). EBI2 expression dominated in mononuclear cells with macrophage-like morphology. Furthermore, immunofluorescence costainings of CD3 with EBI2 showed that a proportion of T cells in MS lesions expressed EBI2 (Figure 7I).

DISCUSSION

Using an EBI2 reporter mouse line, we found that expression of EBI2 in T cells is highly regulated during differentiation. Importantly, differentiation under pro-inflammatory conditions such as exposition to IL-1β and IL-23 supported expression of EBI2 in T cells. In accordance with this "pro-pathogenic" profile of expression, we found that EBI2-deficient encephalitogenic T helper cells showed a delayed kinetic of pathogenicity in transfer EAE compared to WT T cells. We also found that the enzymes generating the EBI2 ligand change their expression dramatically during EAE. Our data therefore support the hypothesis that EBI2 and 7α,25-OHC are part of a system that promotes redirection of inflammatory Th17 cells from secondary lymphoid organs to sites of inflammation.

Analysis of EBI2 expression showed that EBI2 is highly expressed in central memory CD8+ T cells that is in line with previous data from human T cells in which these cells express higher levels of EBI2 than naive or effector memory CD8+ T cells (Hannedouche et al., 2011). Such cells were shown to have a specific role in fast viral defense in secondary infections (Wherry et al., 2003). Recently, it was suggested that EBI2 has a function in egress of T cells from LNs, because immunized CH25H-deficient animals contained enriched numbers of CD44+ effector T cells in draining LNs (Chalmin et al., 2015). This, together with our findings of differential expression of EBI2 in distinct stages of T cell differentiation, may suggest that EBI2 has an important role in T cell re-localization and possibly in LN egress reminiscent of the S1P-S1P receptor system, similar to its role in germinal center B cells. In two different types of co-transfer experiments, we analyzed where encephalitogenic T cells reside either in the active EAE model or in the transfer model, either before EAE or at onset of EAE. In active EAE, we found similar numbers of proliferating effector T cells irrespective of the EBI2 genotype

---

Figure 5. Encephalitogenic T Cells Deficient in EBI2 Show Deficiencies in CNS Immigration

(A) Experimental setup: spleen and dLNs of immunized congenic WT-CD45.1+ (C57BL/6 background) and EBI2EGFP/EGFP (CD45.2+) mice were harvested on day 9 post immunization and cultured for 4 days in the presence of MOG35–55, IL-23, and αIFNγ. Cells were pooled with a ratio of 1:1 for CD45.1/CD45.2 and injected to RAG1−/− hosts, which were analyzed at EAE score 1–2.

(B) Analysis of the transferred CD45.1 and CD45.2 cells in spleen, blood, and CNS.

(C) Quantification of the ratio between CD45.1+ and CD45.2+ cells in spleen, blood, and CNS.

(D) Experimental setup: spleen and LN of D2D2 WT (CD45.2/CD90.1) and D2D2 x EBI2EGFP/EGFP (CD45.2/CD90.2) mice were CD4+ MACSed- and VCT-labeled. Cells were pooled (1:1 ratios) and transferred to congenic WT-CD45.1+ mice. The recipients were immunized on day 1 post transfer and analyzed on day 9 post immunization. We performed one experiment using male donors and acceptors and one using female donors and acceptors.

(E) Flow cytometric analysis of proliferated 2D2 WT and 2D2 x EBI2EGFP/EGFP cells in LN of naive mice and dLN and blood of MOG-CFA immunized mice.

(F) Ratio of the numbers of proliferated transferred cells in dLN and blood. Left: all transferred cells. Right: Th17 cells.
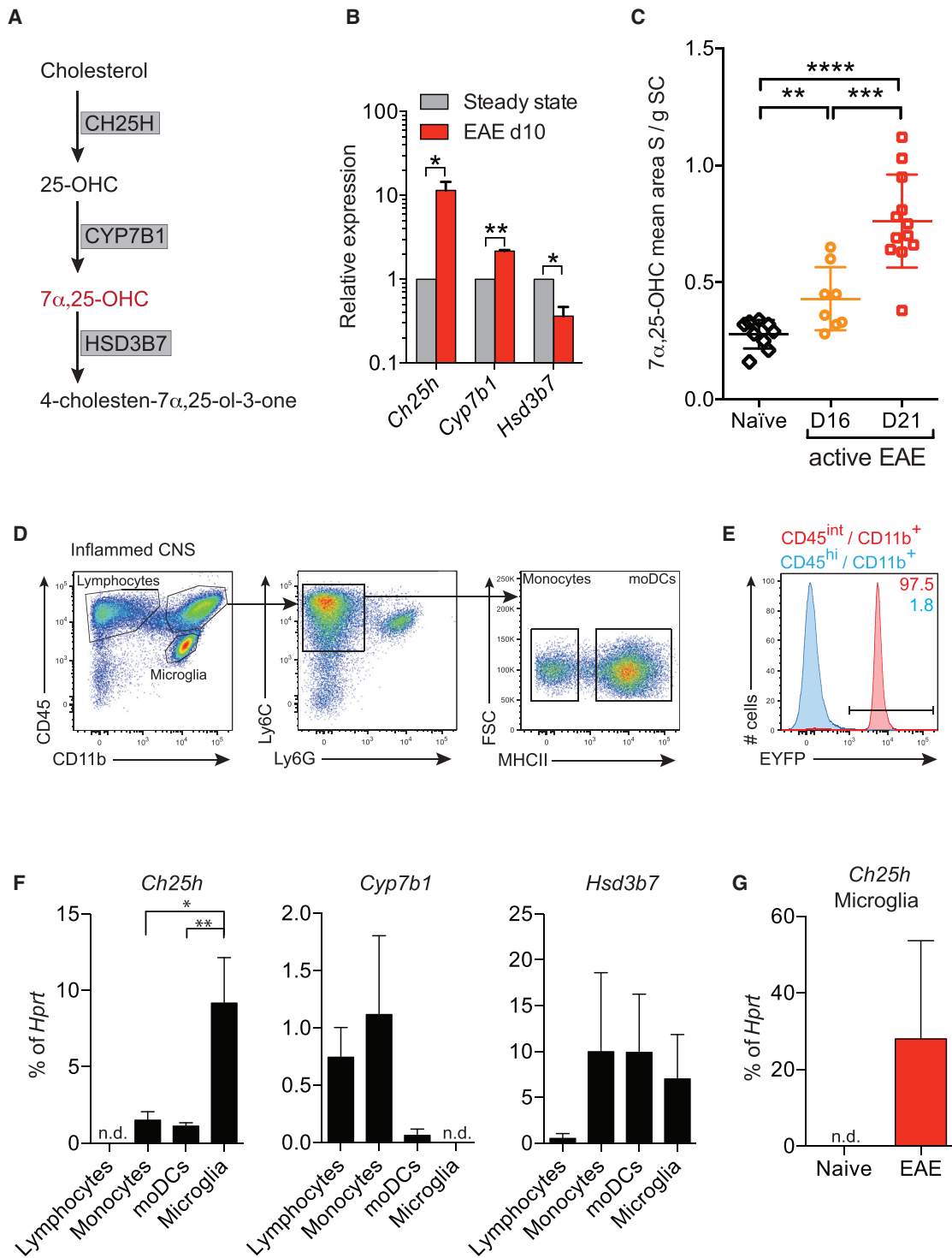
Figure 6. Regulation of 7α,25-OHC Generating Enzymes upon EAE Induction

(A) Metabolic pathway for 7α,25-OHC synthesis from cholesterol. CH25H- and CYP7B1-mediated hydroxylation of cholesterol generates the EBI2 ligand 7α,25-OHC, which is inactivated by HSD3B7.

(B) Expression of *Ch25h*, *Cyp7b1*, and *Hsd3b7* mRNA in SCs of WT mice 10 days after active EAE induction or of naive littermates. Data were normalized to *Hprt* and steady-state condition was set to 1 to compare fold increase or decrease upon EAE induction. Data are representative of two independent experiments (n = 3).

(C) EBI2 ligand in SC of mice with EAE determined by mass spectrometry (tandem MS/MS). SCs from naive mice (n = 9), from mice with EAE at day 16 with low EAE scores (n = 8), and at day 21 post immunization with higher scores (n = 12) were analyzed. Data given is expressed as peak mean area in the chromatogram normalized to the SC tissue weight used in the experiment (mean area S/gram SC tissue).
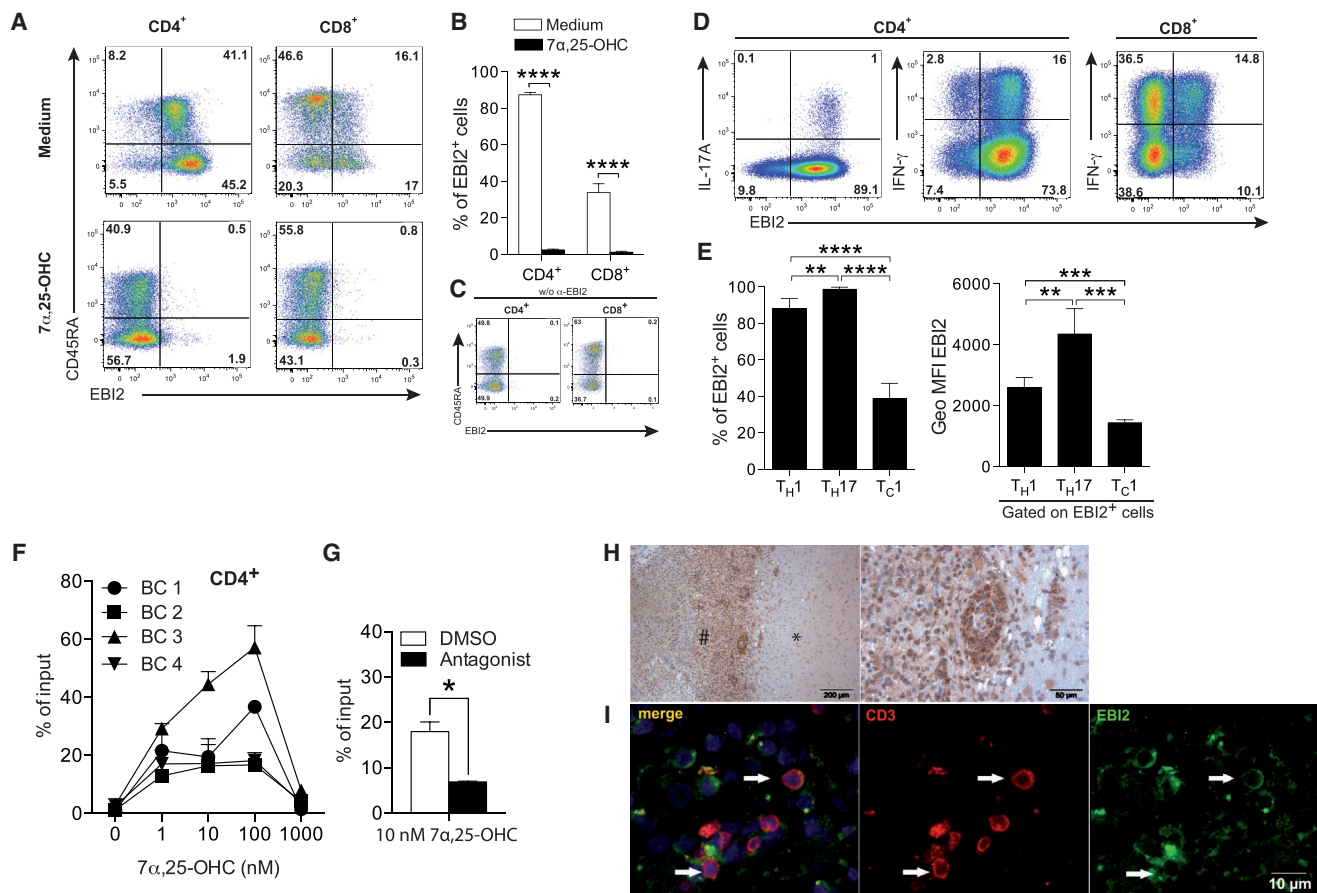
(legend continued on next page)

Figure 7. EBI2 Expression by Human T Cells and Cellular Infiltrates in MS Lesions

(A) EBI2 and CD45RA expression on CD4+/CD8+ T cells of human PBMCs stimulated with 1 μM 7α,25-OHC or left untreated.

(B) Statistical analysis of EBI2+ T cells after stimulation with 1 μM 7α,25-OHC.

(C) Human CD4+/CD8+ T cells stained without addition α-EBI2 antibody, but secondary rabbit α-mouse IgG-biotin and SA-FITC.

(D) Cytokine and EBI2 expression pattern of human CD4+/CD8+ T cells, activated for 5 hr with PMA, ionomycin, and monensin.

(E) Statistical analysis of EBI2+ T cell subsets and respective GeoMFI. Data are representative for at least two independent experiments (n = 5).

(F) Transwell migration assay of α-CD3 and α-CD28 activated PBMCs from four healthy donors toward indicated concentrations of 7α,25-OHC. Migrated CD4+ T cells were quantified by FACS. Shown are means with SD of technical replicates of two independent experiments.

(G) Migration of α-CD3- and α-CD28-activated PBMCs from healthy donors pre-treated with 20 μM EBI2 antagonist NIBR189 or DMSO. Migrated CD4+ T cells were quantified by FACS. Shown are means with SD of technical replicates representative of two independent experiments (n = 3).

(H) Human MS tissue sections were stained with anti-EBI2 (brown). Left: the infiltration of the lesion with numerous EBI2-positive cells (#), whereas in the adjacent periplaque white matter (*) only few positive cells were detected. Right: shows in higher magnification a perivascular infiltrate with numerous EBI2-positive cells.

(I) Immunofluorescence picture of human MS tissue sections stained with anti-CD3 (red), anti-EBI2 (green), and DAPI (blue). In the left panel, the overlay of all colors is shown. Arrows, CD3+ T cells expressing EBI2.

in draining LNs but an accumulation of EBI2-deficient T cells in the blood. In the transfer model, we found a clear ratio change of EBI2-expressing T cells over EBI2-deficient T cells from periphery to the CNS in early EAE. Both experiments point to a role of EBI2 and its ligand in CNS extravasation. Therefore, our data do not support the hypothesis that EBI2 plays a major role in the regulation of T cell LN egress but also does not exclude that certain T cell subpopulations might be differentially

(D) Gating strategy to sort indicated cell populations from the inflamed CNS. Plots are representative for at least four independent experiments.

(E) Cx3cr1CreER x EYFP reporter mice 8 weeks after tamoxifen treatment were subjected to EAE, and indicated cell populations from the CNS were analyzed for EYFP expression. Histogram is representative of two independent experiments.

(F) Expression of *Ch25h*, *Cyp7b1*, and *Hsd3b7* mRNA in indicated cell populations sorted from the CNS of Cx3cr1CreER x EYFP mice with EAE. Data are representative of two independent experiments (n = 2).

(G) Expression of *Ch25h* mRNA in sorted microglia from the CNS of naive mice or animals with EAE. Data are representative for two independent experiments (n = 2).

released of draining lymph nodes (dLNs) after priming in absence of EBI2.

In accordance with its original discovery, EBI2 may play its major role in response to viral infections or in a pathological context such as in autoimmunity. Although we found a significant delay of onset in the Th17 transfer EAE model, active EAE was unchanged in absence of EBI2. At the moment, we can only speculate about this difference. It might be that active EAE induction using CFA/MOG induces a stronger inflammatory array of immune cells, pro-inflammatory factors, cytokines, and chemokines, which might override the need for EBI2-mediated migration. Alternatively, there might be compensatory mechanisms for the lack of this GPCR, so that mice are susceptible to EAE also independently of EBI2 in knockout animals. We showed in transfer experiments with EBI2 mutant T cells that EAE was significantly delayed but after onset, disease proceeded normally. This might be due to the previously described plasticity of Th17 cells, which tend to change their expression profile toward the Th1 lineage together with high levels of GM-CSF (Hirota et al., 2011; Kurschus et al., 2010) (and herein). In absence of EBI2, EAE initiation may more depend on Th1 cells co-expressing GM-CSF than on Th17 cells. This hypothesis is supported by our data showing a major population of Th1 cells co-expressing GM-CSF in the CNS during disease.

We found that Th17 cells, derived either from in vivo immunization or in vitro polarization under pathogenic conditions (in presence of IL-23 and/or IL-1β) expressed high levels of EBI2. In contrast, Th17 cells that were generated in absence of IL-23 or IL-1β lost EBI2 expression during differentiation. Addition of various cytokines revealed that IL-2 was the strongest in promoting down-modulation of EBI2 (data not shown). This result is in line with the inhibitory action of IL-2 on Th17 development (Laurence et al., 2007). Our data are also in line with a previous report showing that *Gpr183* is specifically upregulated in Th17 differentiation under pathogenic conditions (using medium containing TGF-β3) (Lee et al., 2012). Hence, EBI2 expression seems to be part of a pathogenic T cell signature and, based on our results with the Th17-mediated EAE transfer model, we suggest that EBI2 confers pathogenicity to encephalitogenic T cells by enhancing migration into the inflamed CNS.

In mice, our EBI2^{EGFP} reporter showed that EBI2 is expressed consistently in naive T helper cells. Already single positive CD4$^+$ thymocytes express EBI2 (not shown). In effector and regulatory T cells in naive mice, the percentage of EBI2 expression was lower (~40%). Like others (Liu et al., 2011), we found that for efficient in vitro migration, polyclonal pre-stimulation of the T cells was needed (not shown). Our findings that 2D2 cells up-regulate EBI2 in vivo during priming is in line with enhanced levels of EBI2 expression necessary for directed migration toward 7α,25-OHC. Concomitant with a function of EBI2 for effector cell migration, human CD45RO$^-$ memory/Teff cells expressed higher surface EBI2 protein than naive T helper cells. Our data indicate that EBI2 is one of several molecules mediating migration of T cells into the inflamed CNS. Because other important molecules for tissue infiltration, such as CD44, VLA4, and LFA1, are not expressed on naive T cells, those cells may be precluded from immigration to the inflamed CNS despite expression of EBI2.

Here, we show that enzymes responsible for synthesis of 7α,25-OHC from cholesterol are highly expressed in the CNS of mice in response to EAE induction. This was paralleled by increased levels of the EBI2 ligands 7α,25-OHC and 7α,27-OHC in SCs of mice with EAE. Therefore, we suggest that during inflammation, expression of CH25H and CYP7B1 sustain lymphocyte accumulation at sites of inflammation/infection. It has been suggested that expression of CH25H supports transmigration of activated CD44$^+$ T helper cells into activated tissues such as the inflamed CNS. Similarly to our data obtained from the EAE transfer model, the lack of CH25H delays onset of EAE with similar end scores and similar infiltration and demyelination at the end of the experiments (Chalmin et al., 2015). Bone marrow chimeric experiments by the same group suggested that CH25H was needed to be expressed in cells of hematopoietic origin (supposedly monocytes/macrophages or moDCs) rather than in cells of the CNS tissue itself to promote EAE development. Contrary to this, we found that *Ch25h* is expressed by CNS-derived microglia in EAE and not by infiltrating myeloid cell populations. Interestingly, the second enzyme for generating 7α,25-OHC CYP7B1 was expressed by infiltrating lymphocytes and monocytes. This suggests that activated microglia and infiltrating cells have to cooperate in production of the cell-permeable ligand as it was demonstrated previously for different cell lines expressing these enzymes separately (Yi et al., 2012). We did not define the lymphocyte population expressing CYP7B1. Interestingly, NK cells can express this enzyme (Liu et al., 2011) and were also shown to infiltrate the CNS in EAE (Huang et al., 2006). We also did not analyze astrocytes for expression of these enzymes in EAE. It was recently shown that microglia (Butovsky et al., 2014; Olah et al., 2012) as well as murine astrocytes can express the necessary enzymes for production of the EBI2 ligand (Rutkowska et al., 2015, 2016). Alternative sources for EBI2 ligand production in EAE under investigation by us may be endothelial cells. How microglia cells become activated to express *Ch25h* in EAE is not clear. Because we observe major differences in transfer EAE of Th17 cells, we assume that expression of *Ch25h* is not a response to CFA used in active EAE induction but rather induced by inflammatory cytokines.

Interestingly, our analyses of human PBMCs using a monoclonal antibody against EBI2 showed that the expression pattern of human EBI2 is largely overlapping with that in mice. Especially Th17 cells showed homogeneous high expression of EBI2 compared with Th1 cells, which contained a fraction of cells negative for EBI2. Furthermore, when we analyzed histological sections of lesions from MS patients, we found expression of EBI2 restricted to mononuclear cells present within inflamed white matter regions. Most cells expressing EBI2 morphologically appeared as infiltrating macrophages. We found T cells that were clearly negative and T cells with strong expression of EBI2 in MS lesions. This finding is in accordance with our flow cytometry data showing that only a part of all T cells express EBI2 and the fact that MS lesions are known to be dominated by CD8 cells (Babbe et al., 2000), which are largely negative for EBI2.

Because EBI2 is expressed on the major subsets of immune cells, and small molecule antagonists for EBI2 were recently described (Benned-Jensen et al., 2013; Gessier et al., 2014), EBI2 constitutes a tempting drug target reminiscent of the

sphingosine-1-phosphate receptor superagonist *fingolimod*/ Gilenya that is currently in clinical use for treatment of MS patients.

EXPERIMENTAL PROCEDURES

Detailed descriptions about mass spectrometry, single cell RT-PCR, and immunohistochemistry are provided in the Supplemental Information.

Mice

Conditional EBI2^fl-EGFP mice were generated from 129/Ola-derived targeted ES cells (IB10) injected into C57BL/6J blastocysts. Germline transmitted EBI2^fl-EGFP mice were crossed to the Cre deleter strain to generate EBI2-deficient *EBI2*^EGFP/EGFP mice. In the latter animals, the Egfp reporter gene replaces the single coding exon of *Gpr183*, placing the reporter gene under the transcriptional control of the *Gpr183* locus. *EBI2*^EGFP mice used in this study were backcrossed at least eight times onto the C57BL/6J genetic background. Other mouse strains used in the study included 2D2 mice congenic for CD90.1, congenic CD45.1 mice, and RAG1$^{-/-}$ mice, which were obtained from in-house breeding. EBI2$^{(-/-)}$ mice were originally purchased from Deltagen (mixed genetic background C57BL/6 x C129) and then backcrossed onto C57BL/6J background for at least ten generations (Chalmin et al., 2015). Cx3cr1^CreER crossed to Rosa-EYFP mice (Bruttger et al., 2015; Yona et al., 2013) were treated with tamoxifen to induce EYFP recombination and expression in myeloid cells. After 8 weeks, only microglia express the reporter protein, and mice were used for EAE and subsequent cell-sorting experiments. All experiments with mice were carried out in accordance with the guidelines of the Central Animal Facility Institution of Mainz and in accordance with relevant laws and guidelines with permission by the state Rhineland-Palatinate.

Active EAE Induction

Mice were immunized subcutaneously at the base of the tail with 100 μg MOG$_{35-55}$ peptide emulsified in CFA with 1.1 mg of heat inactivated *M. tuberculosis*. Two days later, along with immunization, 200 ng of pertussis toxin (Ptx) (Sigma-Aldrich) was administered by intraperitoneal (i.p.) injection. Mice were scored for signs of EAE as described (Huppert et al., 2010).

Transfer EAE

Mice were immunized as described for active EAE without Ptx. On day 10 post immunization, cells from spleen and LNs were prepared and cultured in TCM with 50 μg/mL MOG$_{35-55}$, 10 μg/mL α-IFN-γ antibodies (BioXCell), and 10 ng/mL IL-23 (Miltenyi) for 4 days at 37°C with 5% CO$_2$. Afterward, 2 × 10^5 blasting Th17 cells were injected intravenously (i.v.) into RAG1$^{-/-}$ mice. Ptx (200 ng) was injected i.p. on the day of T cell transfer and on day 2 post transfer.

Organ Preparation

Single-cell suspensions of LNs and spleens were prepared non-enzymatically in Dulbecco's phosphate buffered saline with 2% fetal calf serum (FCS). For isolation of lymphocytes from the CNS, brain and SC were cut and digested for 20 min at 37°C with 1 mg/mL collagenase II (Sigma) and 40 μg/mL DNase I (Roche) followed by centrifugation in a Percoll gradient (Cardona et al., 2006). Spinal cord for mass spectrometry was isolated from Dulbecco's phosphate buffered saline (DPBS)-perfused animals, dry-frozen in liquid nitrogen, and kept at −80°C or lower until prepared and measured (Supplemental Experimental Procedures). Two independent groups of mice with EAE from different labs were used for spinal cord isolation, one group at day 16 and one at day 21 of EAE.

In Vitro T Cell Differentiation

Naive CD4$^+$ T cells were isolated from spleen and LNs by MACS purification (Miltenyi Biotec) according to the manufacturers protocol. Cells were cultured at 1 × 10^5 cells/well in 200 μL T cell medium (TCM) (RPMI with 10% FCS, 2 mM L-Gln, 100 U/mL penicillin, 100 mg/mL streptomycin, 1 mM sodium pyruvate, 50 mM 2-mercaptoethanol, 10 mM HEPES, and 1% non-essential amino acids

[MEM]) in 96-well plates. For Th1 differentiation, 1 μg/mL α-CD3, 6 ng/mL α-CD28 (BioXCell), and 4 ng/mL IL-12 (Promocell) were used. For Treg differentiation, 1 μg/mL α-CD3 and 10 μg/mL α-IFN-γ antibodies (BioXCell) with 4 ng/mL TGF-β1 (R&D) and 10 ng/mL IL-2 (Promocell) were used. For Th17 differentiation, 1 μg/mL α-CD3, 6 ng/mL α-CD28, and 10 μg/mL α-IFN-γ antibodies (BioXCell) with 2 ng/mL TGF-β1 (R&D) or 100 ng/mL IL-1β (R&D), 5 ng/mL IL-6 (Promocell), and 20 ng/mL IL-23 (Miltenyi) were used. Cells were cultured at 37°C and 5% CO$_2$ for 3 days for Th1 and iTreg differentiation and for 5 days for Th17 differentiation. To study EBI2-EGFP expression during proliferation, MACS-purified CD4$^+$ T cells from EBI2$^{+/EGFP}$ mice were labeled with violet cell tracer (VCT) (Invitrogen) according to the manufacturer's protocol.

Human PBMCs

Buffy coats of healthy human donors who gave their informed consent were obtained from the Center for Blood Transfusion University Medical Center Mainz, Germany. PBMCs were isolated by Ficoll-Hypaque gradient centrifugation.

Flow Cytometry

Antibodies were purchased from eBioscience, BD, and BioLegend. For intracellular cytokine staining, cells were activated for 4 hr in TCM with 50 ng/mL phorbol-12-myristate-13-acetate (PMA), 500 ng/mL ionomycin and 1× monensin (eBioscience) at 37°C and 5% CO$_2$. All incubations were performed on ice or at 4°C in the dark in PBS containing 0.5% BSA and 0.02% NaN$_3$. Prior to surface staining, cells were pretreated with 5 μg/mL FC-Block (BioXCell). Cells were fixed with 2% formaldehyde to retain EGFP. Intracellular cytokine stainings were carried out in 1× Perm buffer (BD). For staining of FoxP3 with EGFP retention, 1× Perm buffer (eBioscience) was used, as described earlier by us (Heinen et al., 2014).

Staining of EBI2 on human PBMCs was done in PBS + 5% normal goat serum + 0.02% NaN$_3$. Fc receptors were blocked for 10 min using TrueStain FcX (Biolegend). The mouse IgG2a anti-human EBI2 monoclonal antibody (mAb) clone 57C9B51C9 was from Novartis (Basel). Other antibodies used were from BioLegend. For staining of cytokines, cells were stimulated in X-VIVO15 medium (Lonza) with PMA, ionomycin, and monensin for 5 hr. Fixation and intracellular staining was done as described for murine cells. Acquisition of stained cells was performed on a BD FACS Canto II and FlowJo was used for analysis.

qRT-PCR

RNA from single cell suspensions was isolated by using RNeasy spin columns (QIAGEN). For RNA isolation from whole spleen and SC, tissue was homogenized mechanically in Trizol (Invitrogen) using lysing matrix D with respective homogenizer (MP FastPrep). Afterward, RNA was isolated by phenol-chloroform extraction. First strand cDNA was prepared by using the Superscript II kit (Invitrogen) with random primers, according to the manufacturers protocol. Quantification of *Gpr183*, *Ch25h*, *Cyp7b1*, and *Hsd3b7* mRNA was done by using a SYBR green assay (Invitrogen) with *Hprt* as reference gene as described (Zayoud et al., 2013). Respective primers were purchased from QIAGEN.

Transwell Migration Assay

Splenocytes or CD4$^+$ and CD8$^+$ MACS-purified T cells were activated in TCM overnight with 1 μg/mL α-CD3 and 6 μg/mL α-CD28 antibodies (BioXCell). The chemokines CCL19/CCL21 (BioLegend) were used at 50 ng/mL each, 7α,25-OHC was obtained from Novartis and used at indicated concentrations. Migration assays were done in TCM and 96-well transwell plates (Congstar) with 5-μm pore size. After 2 hr of incubation at 37°C with 5% CO$_2$, cells in the lower wells were analyzed by flow cytometry. Counting beads (Spherotech) were used for quantification. Human PBMC-derived T cells were activated in TCM with 1 μg/mL α-CD3 and 6 μg/mL α-CD28 antibodies overnight. Afterward, migration assays were performed as described above. Instead of TCM, RPMI 1640 with 0.1% BSA was used and cells were incubated for 3 hr. For some experiments, cells were pretreated with 20 μM of the EBI2 antagonist NIBR189 (Novartis) or DMSO prior to migration.

In Vivo Migration of T Cells

CD4^{+} and CD8^{+} T cells were MACS purified from spleen and LNs of EBI2-deficient mice or WT littermates. Cells (5×10^6) were transferred i.v. into congenic CD90.1[+] mice. After 4 hr, mice were sacrificed and transferred T cells in the spleen and LNs were analyzed and quantified via flow cytometry.

In Vivo T Cell Priming

T helper cells were MACS -purified from spleen and LNs of 2D2 x CD90.1 mice and labeled with CFSE according to the manufacturers protocol. Cells (5×10^6) were transferred i.v. into either EBI2-deficient mice or WT littermates. One day after transfer, mice were immunized s.c. with 100 μg MOG$_{35-55}$ emulsified in complete Freund adjuvant (CFA) or left untreated. Five days after immunization, mice were sacrificed and spleen and LN cells were analyzed via flow cytometry. For other experiments, T helper cells were purified from 2D2 x EBI2$^{+/EGFP}$ or 2D2 x EBI2$^{EGFP/EGFP}$ (CD90.2 background) mice and transferred into congenic CD90.1[+] animals.

Statistics

Graphs were made by using GraphPad-Prism. Statistical significance was calculated using the unpaired two-tailed t test. Values of $p < 0.0001$, $p < 0.001$, $p < 0.01$, and $p < 0.05$ were marked by four, three, two, and one asterisks, respectively. For analyses of paired values (ratios) between organs such as blood and LNs in the same animals, the paired two-tailed t test was used. Data are represented as mean with SD if not stated otherwise.

SUPPLEMENTAL INFORMATION

Supplemental Information includes Supplemental Experimental Procedures, seven figures, and two tables and can be found with this article online at http://dx.doi.org/10.1016/j.celrep.2017.01.020.

REFERENCES

Acosta-Rodriguez, E.V., Napolitani, G., Lanzavecchia, A., and Sallusto, F. (2007). Interleukins 1beta and 6 but not transforming growth factor-beta are essential for the differentiation of interleukin 17-producing human T helper cells. Nat. Immunol. *8*, 942–949.

Babbe, H., Roers, A., Waisman, A., Lassmann, H., Goebels, N., Hohlfeld, R., Friese, M., Schröder, R., Deckert, M., Schmidt, S., et al. (2000). Clonal expansions of CD8(+) T cells dominate the T cell infiltrate in active multiple sclerosis lesions as shown by micromanipulation and single cell polymerase chain reaction. J. Exp. Med. *192*, 393–404.

Benned-Jensen, T., Madsen, C.M., Arfelt, K.N., Smethurts, C., Blanchard, A., Jepras, R., and Rosenkilde, M.M. (2013). Small molecule antagonism of oxysterol-induced Epstein-Barr virus induced gene 2 (EBI2) activation. FEBS Open Bio *3*, 156–160.

Birkenbach, M., Josefsen, K., Yalamanchili, R., Lenoir, G., and Kieff, E. (1993). Epstein-Barr virus-induced genes: first lymphocyte-specific G protein-coupled peptide receptors. J. Virol. *67*, 2209–2220.

Bruttger, J., Karram, K., Wörtge, S., Regen, T., Marini, F., Hoppmann, N., Klein, M., Blank, T., Yona, S., Wolf, Y., et al. (2015). Genetic cell ablation reveals clusters of local self-renewing microglia in the mammalian central nervous system. Immunity *43*, 92–106.

Butovsky, O., Jedrychowski, M.P., Moore, C.S., Cialic, R., Lanser, A.J., Gabriely, G., Koeglsperger, T., Dake, B., Wu, P.M., Doykan, C.E., et al. (2014). Identification of a unique TGF-β-dependent molecular and functional signature in microglia. Nat. Neurosci. *17*, 131–143.

Cardona, A.E., Huang, D., Sasse, M.E., and Ransohoff, R.M. (2006). Isolation of murine microglial cells for RNA analysis or flow cytometry. Nat. Protoc. *1*, 1947–1951.

Chalmin, F., Rochemont, V., Lippens, C., Clottu, A., Sailer, A.W., Merkler, D., Hugues, S., and Pot, C. (2015). Oxysterols regulate encephalitogenic CD4 T cell trafficking during central nervous system autoimmunity. J. Autoimmun. *56*, 45–55.

Chung, Y., Chang, S.H., Martinez, G.J., Yang, X.O., Nurieva, R., Kang, H.S., Ma, L., Watowich, S.S., Jetten, A.M., Tian, Q., and Dong, C. (2009). Critical regulation of early Th17 cell differentiation by interleukin-1 signaling. Immunity *30*, 576–587.

Croxford, A.L., Lanzinger, M., Hartmann, F.J., Schreiner, B., Mair, F., Pelczar, P., Clausen, B.E., Jung, S., Greter, M., and Becher, B. (2015). The cytokine GM-CSF drives the inflammatory signature of CCR2+ monocytes and licenses autoimmunity. Immunity *43*, 502–514.

Gatto, D., Paus, D., Basten, A., Mackay, C.R., and Brink, R. (2009). Guidance of B cells by the orphan G protein-coupled receptor EBI2 shapes humoral immune responses. Immunity *31*, 259–269.

Gatto, D., Wood, K., Caminschi, I., Murphy-Durland, D., Schofield, P., Christ, D., Karupiah, G., and Brink, R. (2013). The chemotactic receptor EBI2 regulates the homeostasis, localization and immunological function of splenic dendritic cells. Nat. Immunol. *14*, 446–453.

Gessier, F., Preuss, I., Yin, H., Rosenkilde, M.M., Laurent, S., Endres, R., Chen, Y.A., Marsilje, T.H., Seuwen, K., Nguyen, D.G., and Sailer, A.W. (2014). Identification and characterization of small molecule modulators of the Epstein-Barr virus-induced gene 2 (EBI2) receptor. J. Med. Chem. *57*, 3358–3368.

Ghoreschi, K., Laurence, A., Yang, X.P., Tato, C.M., McGeachy, M.J., Konkel, J.E., Ramos, H.L., Wei, L., Davidson, T.S., Bouladoux, N., et al. (2010). Generation of pathogenic T(H)17 cells in the absence of TGF-β signalling. Nature *467*, 967–971.

Hannedouche, S., Zhang, J., Yi, T., Shen, W., Nguyen, D., Pereira, J.P., Guerini, D., Baumgarten, B.U., Roggo, S., Wen, B., et al. (2011). Oxysterols direct immune cell migration via EBI2. Nature *475*, 524–527.

Heinen, A.P., Wanke, F., Moos, S., Attig, S., Luche, H., Pal, P.P., Budisa, N., Fehling, H.J., Waisman, A., and Kurschus, F.C. (2014). Improved method to retain cytosolic reporter protein fluorescence while staining for nuclear proteins. Cytometry A *85*, 621–627.

Hirota, K., Duarte, J.H., Veldhoen, M., Hornsby, E., Li, Y., Cua, D.J., Ahlfors, H., Wilhelm, C., Tolaini, M., Menzel, U., et al. (2011). Fate mapping of IL-17-producing T cells in inflammatory responses. Nat. Immunol. *12*, 255–263.

Huang, D., Shi, F.D., Jung, S., Pien, G.C., Wang, J., Salazar-Mather, T.P., He, T.T., Weaver, J.T., Ljunggren, H.G., Biron, C.A., et al. (2006). The neuronal chemokine CX3CL1/fractalkine selectively recruits NK cells that modify experimental autoimmune encephalomyelitis within the central nervous system. FASEB J. *20*, 896–905.

Huppert, J., Closhen, D., Croxford, A., White, R., Kulig, P., Pietrowski, E., Bechmann, I., Becher, B., Luhmann, H.J., Waisman, A., and Kuhlmann, C.R. (2010). Cellular mechanisms of IL-17-induced blood-brain barrier disruption. FASEB J. 24, 1023–1034.

Kelly, E., Bailey, C.P., and Henderson, G. (2008). Agonist-selective mechanisms of GPCR desensitization. Br. J. Pharmacol. 153 (Suppl 1), S379–S388.

Kurschus, F.C., Croxford, A.L., Heinen, A.P., Wörtge, S., Ielo, D., and Waisman, A. (2010). Genetic proof for the transient nature of the Th17 phenotype. Eur. J. Immunol. 40, 3336–3346.

Laurence, A., Tato, C.M., Davidson, T.S., Kanno, Y., Chen, Z., Yao, Z., Blank, R.B., Meylan, F., Siegel, R., Hennighausen, L., et al. (2007). Interleukin-2 signaling via STAT5 constrains T helper 17 cell generation. Immunity 26, 371–381.

Lee, Y., Awasthi, A., Yosef, N., Quintana, F.J., Xiao, S., Peters, A., Wu, C., Kleinewietfeld, M., Kunder, S., Hafler, D.A., et al. (2012). Induction and molecular signature of pathogenic T(H)17 cells. Nat. Immunol. 13, 991–999.

Li, J., Lu, E., Yi, T., and Cyster, J.G. (2016). EBI2 augments Tfh cell fate by promoting interaction with IL-2-quenching dendritic cells. Nature 533, 110–114.

Liu, G., Yang, K., Burns, S., Shrestha, S., and Chi, H. (2010). The S1P(1)-mTOR axis directs the reciprocal differentiation of T(H)1 and T(reg) cells. Nat. Immunol. 11, 1047–1056.

Liu, C., Yang, X.V., Wu, J., Kuei, C., Mani, N.S., Zhang, L., Yu, J., Sutton, S.W., Qin, N., Banie, H., et al. (2011). Oxysterols direct B-cell migration through EBI2. Nature 475, 519–523.

Olah, M., Amor, S., Brouwer, N., Vinet, J., Eggen, B., Biber, K., and Boddeke, H.W. (2012). Identification of a microglia phenotype supportive of remyelination. Glia 60, 306–321.

Pereira, J.P., Kelly, L.M., Xu, Y., and Cyster, J.G. (2009). EBI2 mediates B cell segregation between the outer and centre follicle. Nature 460, 1122–1126.

Reboldi, A., Dang, E.V., McDonald, J.G., Liang, G., Russell, D.W., and Cyster, J.G. (2014). Inflammation. 25-Hydroxycholesterol suppresses interleukin-1-driven inflammation downstream of type I interferon. Science 345, 679–684.

Rutkowska, A., Preuss, I., Gessier, F., Sailer, A.W., and Dev, K.K. (2015). EBI2 regulates intracellular signaling and migration in human astrocyte. Glia 63, 341–351.

Rutkowska, A., O'Sullivan, S.A., Christen, I., Zhang, J., Sailer, A.W., and Dev, K.K. (2016). The EBI2 signalling pathway plays a role in cellular crosstalk between astrocytes and macrophages. Sci. Rep. 6, 25520.

Suan, D., Nguyen, A., Moran, I., Bourne, K., Hermes, J.R., Arshi, M., Hampton, H.R., Tomura, M., Miwa, Y., Kelleher, A.D., et al. (2015). T follicular helper cells have distinct modes of migration and molecular signatures in naive and memory immune responses. Immunity 42, 704–718.

Wherry, E.J., Teichgräber, V., Becker, T.C., Masopust, D., Kaech, S.M., Antia, R., von Andrian, U.H., and Ahmed, R. (2003). Lineage relationship and protective immunity of memory CD8 T cell subsets. Nat. Immunol. 4, 225–234.

Yi, T., and Cyster, J.G. (2013). EBI2-mediated bridging channel positioning supports splenic dendritic cell homeostasis and particulate antigen capture. eLife 2, e00757.

Yi, T., Wang, X., Kelly, L.M., An, J., Xu, Y., Sailer, A.W., Gustafsson, J.A., Russell, D.W., and Cyster, J.G. (2012). Oxysterol gradient generation by lymphoid stromal cells guides activated B cell movement during humoral responses. Immunity 37, 535–548.

Yona, S., Kim, K.W., Wolf, Y., Mildner, A., Varol, D., Breker, M., Strauss-Ayali, D., Viukov, S., Guilliams, M., Misharin, A., et al. (2013). Fate mapping reveals origins and dynamics of monocytes and tissue macrophages under homeostasis. Immunity 38, 79–91.

Zayoud, M., El Malki, K., Frauenknecht, K., Trinschek, B., Kloos, L., Karram, K., Wanke, F., Georgescu, J., Hartwig, U.F., Sommer, C., et al. (2013). Subclinical CNS inflammation as response to a myelin antigen in humanized mice. J. Neuroimmune Pharmacol. 8, 1037–1047.